

Kent Academic Repository

Full text document (pdf)

Citation for published version

uriš, Miroslav and Bradu, Adrian and Podoleanu, Adrian and Hughes, Michael (2018) Towards an ultra-thin medical endoscope: multimode fibre as a wide-field image transferring medium.

In: Podoleanu, Adrian G.H. and Bang, Ole, eds. 2nd Canterbury Conference on OCT with Emphasis on Broadband Optical Sources. SPIE ISBN 9781510616745.

DOI

<https://doi.org/10.1117/12.2283482>

Link to record in KAR

<http://kar.kent.ac.uk/67071/>

Document Version

Publisher pdf

Copyright & reuse

Content in the Kent Academic Repository is made available for research purposes. Unless otherwise stated all content is protected by copyright and in the absence of an open licence (eg Creative Commons), permissions for further reuse of content should be sought from the publisher, author or other copyright holder.

Versions of research

The version in the Kent Academic Repository may differ from the final published version.

Users are advised to check <http://kar.kent.ac.uk> for the status of the paper. **Users should always cite the published version of record.**

Enquiries

For any further enquiries regarding the licence status of this document, please contact:

researchsupport@kent.ac.uk

If you believe this document infringes copyright then please contact the KAR admin team with the take-down information provided at <http://kar.kent.ac.uk/contact.html>

PROCEEDINGS OF SPIE

[SPIDigitalLibrary.org/conference-proceedings-of-spie](https://spiedigitallibrary.org/conference-proceedings-of-spie)

Towards an ultra-thin medical endoscope: multimode fibre as a wide-field image transferring medium

Miroslav Ďuriš, Adrian Bradu, Adrian Podoleanu, Michael Hughes

Miroslav Ďuriš, Adrian Bradu, Adrian Podoleanu, Michael Hughes, "Towards an ultra-thin medical endoscope: multimode fibre as a wide-field image transferring medium," Proc. SPIE 10591, 2nd Canterbury Conference on OCT with Emphasis on Broadband Optical Sources, 105910A (5 March 2018); doi: 10.1117/12.2283482

SPIE.

Event: Second Canterbury Conference on Optical Coherence Tomography, 2017, Canterbury, United Kingdom

Towards an ultra-thin medical endoscope: Multimode fibre as a wide-field image transferring medium

Miroslav Ďuriš^{a,b}, Adrian Bradu^a, Adrian Podoleanu^a, Michael Hughes^{a,*}

^aApplied Optics Group, School of Physical Sciences, University of Kent, Canterbury,
CT2 7NH, United Kingdom

^bBrno University of Technology, Brno, Czech Republic

ABSTRACT

Multimode optical fibres are attractive for biomedical and industrial applications such as endoscopes because of the small cross section and imaging resolution they can provide in comparison to widely-used fibre bundles. However, the image is randomly scrambled by propagation through a multimode fibre. Even though the scrambling is unpredictable, it is deterministic, and therefore the scrambling can be reversed. To unscramble the image, we treat the multimode fibre as a linear, disordered scattering medium. To calibrate, we scan a focused beam of coherent light over thousands of different beam positions at the distal end and record complex fields at the proximal end of the fibre. This way, the input-output response of the system is determined, which then allows computational reconstruction of reflection-mode images. However, there remains the problem of illuminating the tissue via the fibre while avoiding back reflections from the proximal face. To avoid this drawback, we provide here the first preliminary confirmation that an image can be transferred through a 2x2 fibre coupler, with the sample at its distal port interrogated in reflection. Light is injected into one port for illumination and then collected from a second port for imaging.

Keywords: Multimode fibre, fibre coupler, wide-field imaging, endoscope, endomicroscope, disordered medium, imaging

1. INTRODUCTION

High resolution imaging of human tissue *in vivo* is a rapidly developing field, and offers huge potential advantages over conventional histopathology. Endoscopic microscopes often make use of coherent fibre imaging bundles, containing tens of thousands of fibre cores, to relay images from the tissue to an external imaging system as they are flexible, sub-millimetre in diameter and robust enough for medical use¹. However, while bundles can be passed through the working channel of an endoscope for surface imaging, their diameter is relatively large for mounting inside a needle, which would be necessary to acquire images from beneath the tissue surface. Placing the bundle inside a needle also precludes the use of a distal lens assembly to magnify the bundle face onto the tissue, and so the image resolution is limited to the native resolution of the bundle. With the typical minimum core spacing in bundles being around 3-4 μm , the resolution is therefore limited by Nyquist to 6-8 μm .

There is therefore a need for higher-resolution, smaller-diameter image conduits to improve diagnostic sensitivity while minimising invasiveness and tissue trauma. One potential candidate for forming these image conduits is multimode fibre²⁻⁸. A typical multimode fibre can potentially transmit an order of magnitude more information than a fibre bundle of the same diameter due to the large number of modes it supports⁷. However, due to the different propagation velocity of light coupled into each mode, an image projected onto one end of a multimode fibre will be entirely scrambled when it exits the other.

While unpredictable, this scrambling is repeatable in time providing that the configuration of the fibre is not changed. Hence, if incorporated into a rigid needle, a multimode fibre could act as an image conduit if a prior calibration allows the distortion to be corrected. One approach to this is to use a spatial light modulator (SLM) to generate a series of pre-determined complex light fields at the proximal tip of the fibre which result in a scanned, focused point of light at the distal end²⁻⁶. If all light returning from each focused point is collected, an image can then be assembled. However, since an update of the SLM is required for each point on the image, the approach is necessarily slow.

An alternative technique, developed by Choi et al.^{7,8}, does not require an SLM, and can be used to acquire images through a multimode fibre in a single shot (although multiple images are required in practice to average speckle noise). In this technique, which is similar to the one used in this paper, the transmission matrix of the fibre is first determined by

*m.r.hughes@kent.ac.uk

recording the complex field at the proximal end (for notation see Fig. 3) of the fibre (via digital off-axis holography) in response to a series of plane waves incident on the distal end. Subsequently, when an unknown object is placed at the distal end, it is then possible to obtain a representation of this unknown object in the basis of plane waves by projecting the complex field recorded at the proximal end of the fibre from the unknown object onto the set of pre-recorded calibration complex fields. Once the representation of the object in this basis is known, it is then trivial to convert this to a real-space representation. It should be noted that, unlike the phase conjugation approach described above, this method is only applicable to coherent imaging and cannot be used with fluorescence.

The problem remains of how to illuminate the tissue. In the work of Choi et al.⁷, light was coupled into the multimode fibre from the proximal end, with cross-polarisation used to reject back-reflections from the fibre face. In this paper we instead explore the idea of using a 2x2 fibre coupler to achieve illumination without the problem of back-reflections.

2. METHODS AND EXPERIMENTAL SET-UP

In this section we describe the principles and methods used to exploit properties of multimode fibres and fibre couplers for endoscopic and endomicroscopic imaging. To overcome image distortion (see Fig. 1 left) on the way through the fibre, a prior calibration is required (calibration stage), followed by computational reconstruction in the imaging stage. The approach is based on that originally presented in recent work by Choi et al.⁷, with modifications as detailed below.

We assume that the multimode fibre behaves as a linear, disordered scattering medium. The complex electric field at the distal (tissue) end of the fibre (the object plane), $E_{OP}(\zeta, \eta)$, due to light scattered from an illuminated sample, can be approximately represented as a superposition of idealised point sources,

$$E_{OP}(\zeta, \eta) = \sum_{\zeta', \eta'} A_P(\zeta', \eta') \delta_{\zeta, \zeta'} \delta_{\eta, \eta'}, \quad (1)$$

where δ_{ij} is the Kronecker delta, and $A_P(\zeta, \eta)$ is a complex coefficient carrying information about amplitude and phase at point (ζ, η) . Note that, in Ref 7, the object plane was decomposed into a sum of plane waves (i.e. points in k space) whereas here we work directly with points in real space.

Due to the random scrambling in the fibre, each point source in the object plane, with coordinates (ζ, η) and complex coefficient $A_P(\zeta, \eta)$, results in a corresponding transmitted complex point spread function $E_{tr}(\zeta, \eta; x, y)$ at the image plane at the proximal end of the fibre. Since an arbitrary object can be considered a coherent summation of points at the object plane, the resulting field at the image plane will also be a coherent sum of the corresponding complex point spread functions. Due to the linear behaviour of the fibre, the complex coefficients $A_P(\zeta, \eta)$ are preserved during transmission. Therefore, the output field at the image plane $E_{IP}(x, y)$ can be expressed as a superposition of complex point spread functions multiplied by the same corresponding complex coefficients,

$$E_{IP}(x, y) = \sum_{\zeta, \eta} A_P(\zeta, \eta) E_{tr}(\zeta, \eta; x, y). \quad (2)$$

It is therefore possible to reconstruct the complex field corresponding to any object at the distal end of the fibre if the matrix of transmitted fields $E_{tr}(\zeta, \eta; x, y)$ for each point (ζ, η) at the object plane is known. Critically, provided that the fibre is not disturbed, the transmission matrix $E_{tr}(\zeta, \eta; x, y)$ is constant over time, and can be determined in a calibration prior to imaging, by the method described below. The coefficients $A_P(\zeta, \eta)$, corresponding to the complex field points at the object plane, can then be reconstructed by projection of the image field $E_{IP}(x, y)$ onto the corresponding components of $E_{tr}(\zeta, \eta; x, y)$, which in the ideal case forms an orthogonal basis. This projection operation is repeated for each calibrated point in the object plane to recover the entire image from only a single recorded

complex field at the image plane. If the two-dimensional matrices $E_{IP}(x, y)$ and $E_{tr}(\zeta, \eta; x, y)$ are transformed into vectors then this projection operation can be expressed as a dot product of two vectors:

$$A_p(\zeta, \eta) = E_{IP}(x, y) \cdot E_{tr}(\zeta, \eta; x, y). \quad (3)$$

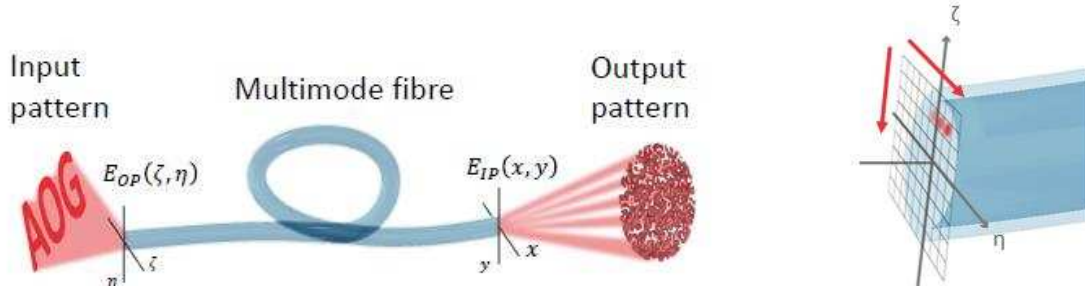


Figure 1. Left – illustration of light scrambling from object plane to image plane in the multimode fibre. Right – calibration step, scanning of a focused laser point over the object plane in a 2D raster pattern.

During the calibration stage, we record the 2D transmitted complex fields (at the proximal end of the fibre) for an array of point sources in the object plane, by scanning a focused laser point over the object plane (distal end of the fibre) in a 2D raster pattern (see Fig. 1 right). This directly provides $E_{tr}(\zeta, \eta; x, y)$. The laser spot at the object plane has a finite size which can be approximated by a two-dimensional Gaussian function. To take this into account in the reconstruction, equation (1) can be then modified as follows:

$$E_{OP}(\zeta, \eta) = \sum_{\zeta', \eta'} A_p(\zeta', \eta') G(\zeta', \eta'), \quad (4)$$

where $G(\zeta', \eta') = (\zeta' - \zeta)^2 / (2\sigma_\zeta^2) + (\eta' - \eta)^2 / (2\sigma_\eta^2)$, and $\sigma_\zeta, \sigma_\eta$ are determined by the measured size of the focused point during calibration. Thus, following the projection operation, equation (4) is used to reconstruct the complex field of the object.

There is a further obstacle to practical endoscopic imaging through multimode fibres. Light can be sent through the fibre to illuminate the tissue, but due to modal interference this lightfield results in a speckle pattern at the object plane. The illumination will not therefore be uniform and the scattered complex field entering back into the fibre will be corrupted by random speckle. Therefore, when the reconstruction of this backscattered light is performed, the final image is again in the form of a speckle image, but with object information imprinted. Fig. 2 illustrates this effect. One solution to this problem is to vary the input field used for illumination resulting in a series of different speckle patterns at the object plane⁷. If images are reconstructed for multiple illumination speckle patterns and incoherently summed, the speckle patterns average out, resulting in a despeckled image. In practice, the order of 100-500 of these images are recorded with different illumination speckle patterns.

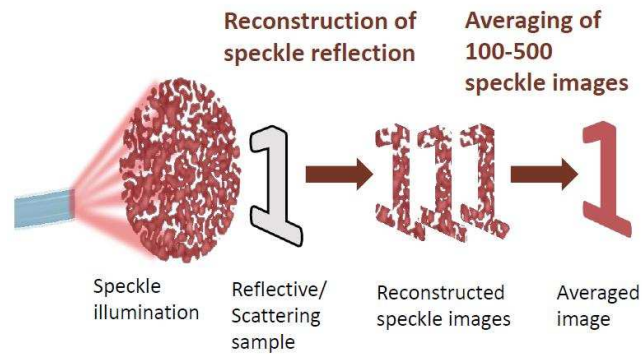


Figure 2. Illumination provided through the multimode fibre and the solution to the nonuniform (speckled) reconstructed images.

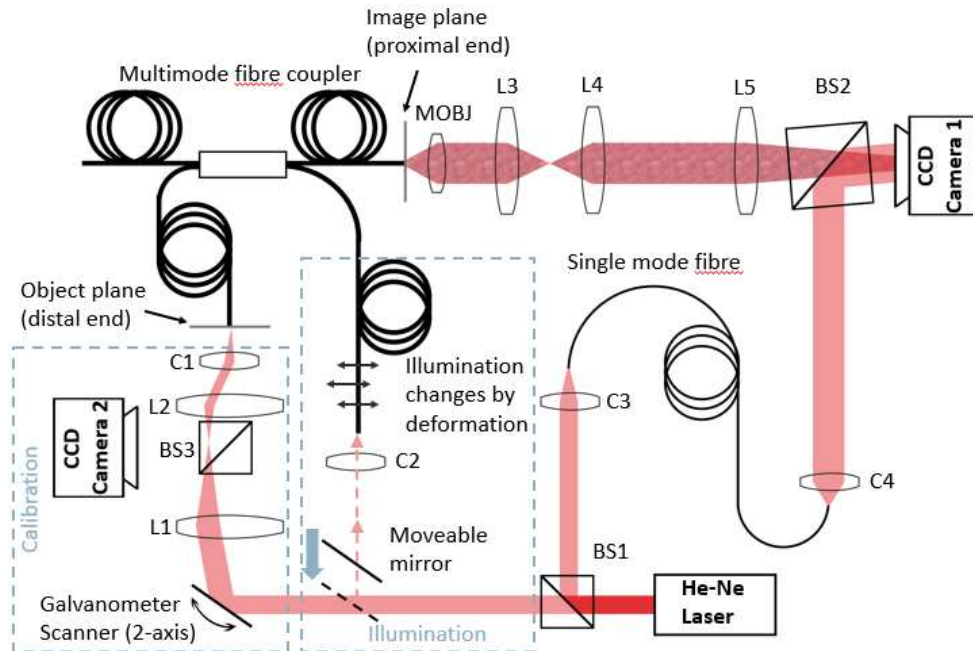


Figure 3. Schematic of the set-up used in our experiments. BS: beam splitter. MOBJ: microscope objective (0.65 NA, 40x). L1: achromatic doublet $f = 50.0$ mm. L2: achromatic doublet $f = 55.0$ mm. C1: Newport Plano-Convex Aspheric lens 0.5 NA, $f = 8.0$ mm, 20x. C2, C3: Newport Plano-Convex Aspheric lens 0.2 NA, $f = 15.3$ mm, 10x. C4: achromatic doublet $f = 19.0$ mm. L3: achromatic doublet $f = 50.0$ mm. L4: achromatic doublet $f = 35.0$ mm. L5: achromatic doublet $f = 100.0$ mm.

Fig. 3 shows the schematic of the set-up used in our experiments. For the reconstruction procedure, we need access to the phase and amplitude at the proximal end of the fibre, which is obtained via a digital off-axis holography algorithm⁹ with a coherent light source (He-Ne Laser, wavelength 632.8 nm, power 5 mW) illuminating a Mach-Zehnder interferometer. The multimode fibre (in our case one path through a multimode fibre coupler) and the object make up the object arm and in the reference arm there is a single mode fibre to match the optical path length. The tip of the proximal end of the fibre is imaged by a system of microscope objective MOBJ, L3 and telescope L4, L5 onto a CCD camera 1 (Allied Vision Guppy F-033B). Beam splitter 2 is tilted so the reference beam is incident on the camera chip at an angle with respect to the multimode fibre axis. This tilt results in an interference pattern. The complex field at the proximal end of the fibre can then be recovered by the off-axis holography technique⁹.

The calibration procedure is performed using a 2-axis galvanometer scanning head and a set of lenses L1, L2, C1 to focus and scan the beam over the distal fibre end. Beam splitter 3 and CCD camera 2 in the calibration part of the set-up are used purely to facilitate adjustment of the fibre, lenses and the object during measurements. This part of the set-up also provides the information about the size of the focused point during the calibration stage. Following calibration, the

entire calibration set-up could, in principle, be removed. We used a multimode fibre coupler (Thorlabs, Inc, fused 2x2, fibre type: FT200UMT, step-Index, 0.39 NA, Ø200 µm core, each arm 1 m long) for object illumination and image transmission. The transmission matrix of the fibre is calibrated using the procedure described above, whereby a spot is focused at multiple positions on the distal end of the fibre (using the galvo scanners) and the complex field at the proximal end is then recorded by the digital holography set-up for each calibration point.

The third arm of the coupler, as shown in Fig. 3, is used purely for illumination purposes during the imaging stage. After the calibration is complete, the moveable mirror is moved into the beam from the laser, switching the operation regime from Calibration to Measurement, so that the non-calibrated arm of the fibre coupler is then illuminated. In this way, light is delivered to the distal end of the fibre coupler, illuminating the object. It is then possible to record images in reflection mode. To average out the speckled illumination patterns, we manually deform the noncalibrated part of the fibre coupler while acquiring a stack of images, so that the illumination speckle pattern changes between each image. Each image is then individually reconstructed, and the resulting intensity images are summed incoherently to produce a final intensity image. The fourth arm of the coupler is not used.

3. RESULTS AND DISCUSSION

To verify our assumptions and methods proposed in the previous section, we first imaged a USAF resolution target through a separate multimode fibre (Thorlabs, Inc, fibre type: FT200EMT, step-Index, 0.39 NA, Ø200 µm core, 1 m long) in transmission mode. This fibre replaced the coupler shown in Fig. 3, running from the marked distal end to the marked proximal end. The object (USAF target) was illuminated by a plane wave at the object plane with the use of the calibration part of the set-up, and the image transmitted through the fibre was recorded. Fig. 4 shows examples of the reconstructed images. Images were obtained by summing 5 reconstructed amplitude images acquired with slightly different illumination angles (varied by adjusting the galvo scanners). These measurements of the USAF target provide information about the resolution of the system in transmission mode. In the images shown it is possible to resolve features of USAF target group 7 up to element 4. This means that the resolution of the system was approximately 6 µm, which is some way below the theoretical resolution limit, determined by the fibre numerical aperture¹⁰, of approximately 1.5 µm. While in this case the resolution was also limited by the use of only 80x80 calibration points to around 5 µm by Nyquist sampling, increasing the number of points did not appear to improve the resolution further.

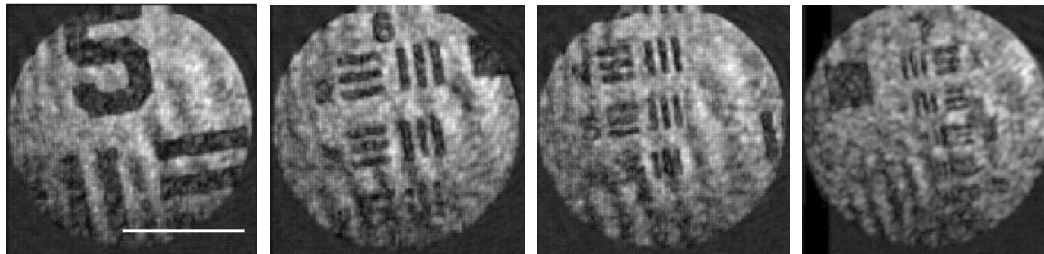


Figure 4. Reconstructed images of the USAF target imaged through a separate multimode fibre in transmission mode. The calibration grid for the scanning protocol was set to 80x80 points, and the diameter (full width at half maximum) of the scanned focused laser spot was 2 µm. Scale bar: 100 µm.

To determine the impact of introducing a fibre coupler, which may include information loss due to effects such as mode coupling and energy loss in individual modes, we performed a comparison of images obtained in transmission mode using the separate multimode fibre and the images obtained using the multimode fibre coupler. Fig. 5 shows images without any postprocessing or corrections made. These images were used to compute the contrast-to-noise ratio defined by the formula:

$$CNR = 20 \log_{10} \left(\frac{A_S}{\sigma_N} \right), \tag{5}$$

where A_S is defined as the difference between the average signal value and the average noise value, and σ_N is the standard deviation of the noise. For the USAF resolution target images, the following results were obtained: $CNR_{\text{fibre}} = 11.0 \text{ dB}$ and $CNR_{\text{coupler}} = 4.9 \text{ dB}$.

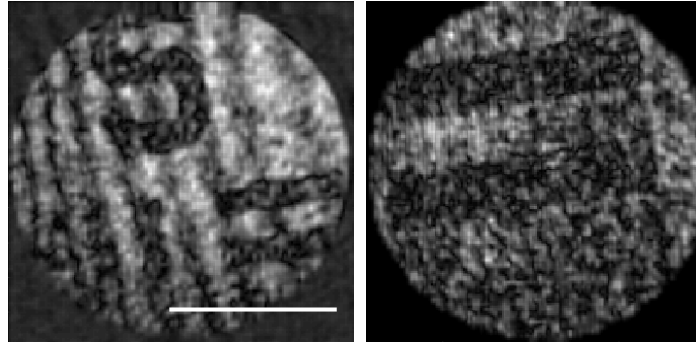


Figure 5. Left – imaging through the separate multimode fibre, Right – imaging through the multimode fibre coupler. Both images were taken in transmission mode without any data postprocessing. The calibration grid for the scanning protocol was set to 80x80 points, and the diameter (full width at half maximum) of the scanned focused laser spot was 2 μm . Scale bar: 100 μm .

An implicit assumption of the reconstruction procedure is that the phase and amplitude, i.e. coefficients $A_{\text{p}}(\zeta, \eta)$, of the scanned focused point is constant throughout the calibration process. This may not be true, and hence the recorded speckle images forming the transmission matrix may need an additional correction for phase and amplitude fluctuations. This can be achieved, in principle, by projecting a plane wave on the distal end of the fibre, and reconstructing this image. Elements of transmission matrix $E_{\text{tr}}(\zeta, \eta; x, y)$ are then divided by the $A_{\text{p}}(\zeta, \eta)$ coefficients computed in the previous step. This correction improves image quality in general, but also introduces artefacts, in that some of the pixels in the reconstructed image have obviously incorrect high amplitude values, and so it can be assumed that these pixels are incorrectly reconstructed. Fig. 6 shows example of corrected images, where red-coloured pixels indicate incorrect reconstruction of object points. The number of these points in the image obtained with the multimode fibre coupler (right) is approximately three times higher than in the left image, obtained with the separate multimode fibre.

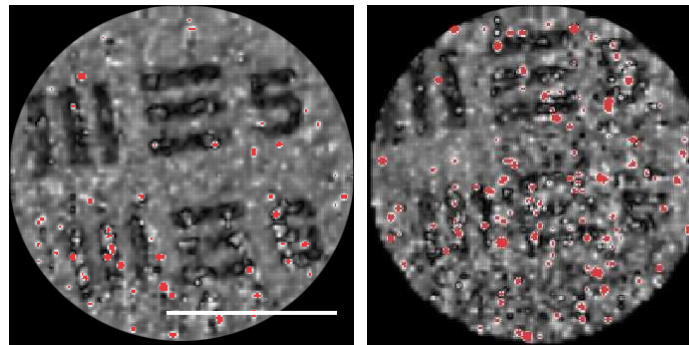


Figure 6. Left – imaging through the separate multimode fibre, Right – imaging through the multimode fibre coupler. Both images were taken in transmission mode. The calibration grid for the scanning protocol was set to 80x80 points, and the diameter (full width at half maximum) of the scanned focused laser spot was 2 μm . Scale bar: 100 μm .

Fig. 7 shows images of a USAF target obtained using the full set-up and proposed method for reflection mode imaging. Averaging was carried out on 100 images reconstructed for different speckle illumination patterns. In the images shown it is possible to resolve features of USAF target group 6 up to element 4. This means that the resolution of our system was approximately 12 μm , which is again significantly below the theoretical resolution limit determined by the fibre numerical aperture of approximately 1.5 μm .

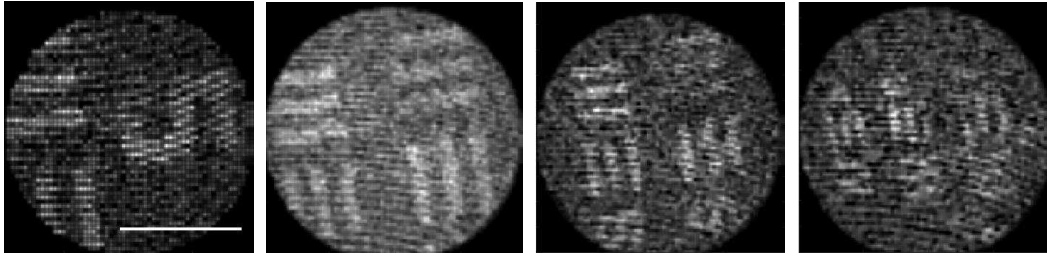


Figure 7. Reconstructed images of USAF target, used for determination of transversal resolution of the set-up in reflection mode. The calibration grid for the scanning protocol was set to 80x80 points, and the diameter (full width at half maximum) of the scanned focused laser spot was 2 μm . Scale bar: 100 μm .

4. CONCLUSIONS

We have shown the first proof-of-concept for image transmission through a fibre coupler and compared this with image transmission through a separate multimode fibre. Image quality through the coupler was lower than image quality through the separate fibre alone, which may be attributable to increased mode coupling or other effects. Incoherent summation when imaging in reflection mode helps to average out the speckled illumination pattern as well as reducing other sources of random noise. Further work is required to perform a more rigorous comparison of image quality in different configurations, to better understand the effects of the fibre coupler on the image reconstruction approach, and to improve the resolution to nearer the theoretical value.

ACKNOWLEDGEMENTS

M. Ďuriš was an intern at the Applied Optics Group at the University of Kent supported by the Erasmus+ traineeship scheme, as part of his master studies at Brno University of Technology. A. Bradu, A. Podoleanu and M. Hughes acknowledge the support of REBOT EPSRC EPN0192291. A. Podoleanu is also supported by the ERC (<http://erc.europa.eu>) AdaSmartRes 754695, NIHR Biomedical Research Centre at Moorfields Eye Hospital NHS Foundation Trust - UCL Institute of Ophthalmology and by the Royal Society Wolfson Research Merit Award.

REFERENCES

- [1] Jabbour, J.M., Saldua, M.A., Bixler, J.N. and Maitland, K.C., "Confocal endomicroscopy: instrumentation and medical applications," *Ann. Biomed. Eng.* 40(2), 378-397 (2012).
- [2] R. N. Mahalati, D. Askarov, J. P. Wilde, and J. M. Kahn, "Adaptive control of input field to achieve desired output intensity profile in multimode fiber with random mode coupling," *Opt. Express* 20, 14321-14337 (2012).
- [3] Papadopoulos, I.N., Farahi, S., Moser, C. and Psaltis, D., "Focusing and scanning light through a multimode optical fiber using digital phase conjugation," *Opt. Express* 20(10), 10583-10590 (2012).
- [4] Čižmár, T. and Dholakia, K., "Exploiting multimode waveguides for pure fibre-based imaging," *Nat. Commun.* 3, 1027 (2012).
- [5] Loterie, D., Farahi, S., Papadopoulos, I., Goy, A., Psaltis, D. and Moser, C., "Digital confocal microscopy through a multimode fiber," *Opt. Express* 23(18), 23845-23858 (2015).
- [6] Plöschner, M., Tyc, T. and Čižmár, T., "Seeing through chaos in multimode fibres," *Nat. Photonics* 9(8), 529-535 (2015).
- [7] Choi, Y., Yoon, C., Kim, M., Yang, T. D., Fnag-Yen, C., Dasari, R. R., Lee, K. J. and Choi, W., "Scanner-Free and Wide-Field Endoscopic Imaging by Using a Single Multimode Optical Fiber," *Phys. Rev. Lett.* 109, 203901 (2012).
- [8] Choi, Y., Yoon, C., Kim, M., Choi, W. and Choi, W., "Optical imaging with the use of a scattering lens," *IEEE J. Sel. Top. Quantum Electron.* 20(2), 61-73 (2014).
- [9] Kreis, T., "Digital holographic interference-phase measurement using the Fourier-transform method," *J. Opt. Soc. Am. A* 3(6), 847-855 (1986).
- [10] Mahalati, R.N., Gu, R.Y. and Kahn, J.M., "Resolution limits for imaging through multi-mode fiber," *Opt. Express* 21(2), 1656-1668 (2013).